HORIBA Scientific

JOBIN YVON Technology

Surface Plasmon Resonance imaging

# Validation of the activity of G-protein-coupled receptors (GPCRs) using SPRi

Application Note
Biology
AN SPRi 32

S. Cortes[a], N. Vollmer[b], K. Mercier[b], A. Abadie[a], B. Tillier[a], C. Frydman[b]

(a) Synthelis, La Tronche, France
(b) HORIBA Scientific, Palaiseau, France

## Introduction

G-protein-coupled receptors (GPCRs), the largest family of integral membrane proteins, participate in the regulation of many physiological functions and are considered as one of the most successful therapeutic targets for a broad spectrum of diseases (approximately 30% of currently marketed drugs). However, despite their pharmacologic potential, clinically useful ligands do not exist for the majority of GPCRs. GPCRs are extremely hydrophobic, characterized by seven transmembrane-spanning $\alpha$-helices. These receptors require a lipid environment to maintain the native structure, conformation and activity. Typically, GPCRs are expressed with low levels in native tissues.

The first challenge in the study of the binding activity of GPCRs is the development of a suitable expression system to correctly produce these proteins. A cell-free expression system has been developed and optimized by Synthelis for producing folded membrane proteins into liposomes to form proteoliposomes.

The second challenge is the development of biochemical or biophysical protocols to measure GPCR-ligand interactions. Surface Plasmon Resonance imaging (SPRi) represents an ideal method to directly study GPCR-ligand interactions. Also, this technology offers the opportunity for high-throughput label-free screening. The bottleneck is the immobilization of proteoliposomes containing membrane proteins to the sensor surface, conditions that retain the active conformation of the protein. Ligand binding is a good indication of correct conformation of a membrane protein.

We have developed a GPCR biosensor assay protocol using as model a Chemokine Receptor type 4 (CxCR4) which has great potential in drug therapy development. CxCR4 is involved in many diseases including cancer and immunodeficiency disorders. The functional proteoliposomes CxCR4 was tested by the binding of native chemokine ligand stromal cell-derived factor 1$\alpha$ (SDF1-1$\alpha$) and two others specific ligands (injected molecules).

## Materials and Methods

### Cell-free expression of the GPCR

Synthelis has developed a technological platform allowing the expression of large quantities of full length membrane proteins in a custom cell-free expression system in a proteoliposome format (GPCRs, Ion Channels, Transporters, Receptors,…), while keeping their structural and functional integrity.

CxCR4 chemokine receptor has been expressed directly from the Synthelis cell-free system into the customized lipid bilayer of liposomes. Then the CxCR4 receptors were identified by Western blot, and quantified using Coomasie Blue staining (figure 1).

Figure 3 shows the image of the spotted biochip and the spotting map.

| | | | | |
|---|---|---|---|---|
| CxCr4 3.12 µg/mL | CxCr4 3.12 µg/mL | CxCr4 3.12 µg/mL | CxCr4 3.12 µg/mL | CxCr4 3.12 µg/mL |
| CxCr4 6.25 µg/mL | CxCr4 6.25 µg/mL | CxCr4 6.25 µg/mL | CxCr4 6.25 µg/mL | CxCr4 6.25 µg/mL |
| CxCr4 12.5 µg/mL | CxCr4 12.5 µg/mL | CxCr4 12.5 µg/mL | CxCr4 12.5 µg/mL | CxCr4 12.5 µg/mL |
| CxCr4 25 µg/mL | CxCr4 25 µg/mL | CxCr4 25 µg/mL | CxCr4 25 µg/mL | CxCr4 25 µg/mL |
| NC | NC | NC | NC | NC |
| Avidine | Avidine | Avidine | Avidine | Avidine |

*Figure 3: Spotting map and image of the spotted molecules matrix on the SPRi-Biochip™.*

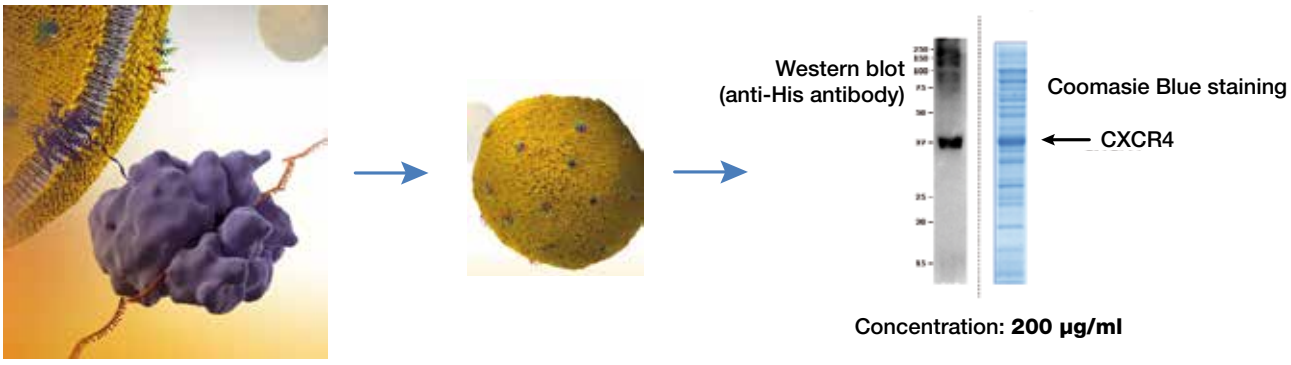


*Patent : WO 2008152262 A2 (Formation de protéoliposomes contenant des protéines membranaires, à l'aide d'un système de synthèse protéique acellulaire)*

*Figure 1: Direct expression of MPs into customized lipid bilayer and CxCR4 identification by Western-blot and CxCR4 quantification using Coomasie Blue staining in the proteoliposomes.*

### Immobilization of biotinylated CxCR4 proteoliposome on a SPRi-Biochip™

First, the electropolymerized avidin-pyrrole spots (STEP 1) were carried out in order to immobilize proteoliposomes on a SPRi-Biochip™. Then two biotinylated proteoliposomes were spotted at 0.93, 2.77, 8.33 and 25 µg/mL on avidin-pyrrole spots using the SPRi-Arrayer (STEP 2).

The first one is a biotinylated CxCR4 proteoliposome (Synthelis, France) and the second one is a negative control, a proteoliposome containing a non-relevant protein (Synthelis, France) which does not react with the injected analytes.

The figure 2 represents the principle of the immobilization.

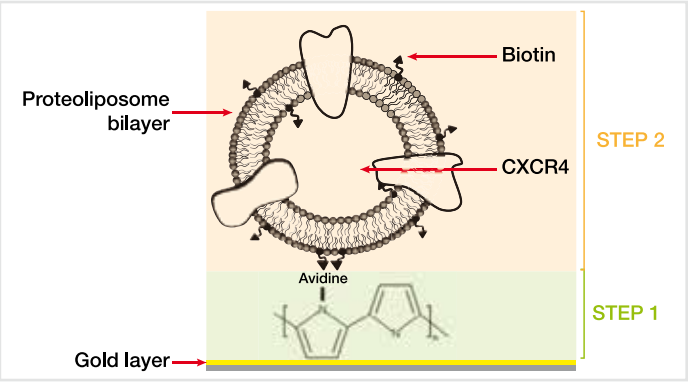


*Figure 2: Immobilization steps. Liposomes containing trace amounts of biotinylated lipids are retained on the surface via covalently attached avidin.*

### Features of injected ligands

The demonstration of a correct conformation is achieved by observing the binding of different ligands to CxCR4. The choice of ligands depends on the binding site. These ligands recognize different epitopes of CxCR4 receptor. Three ligands were successively injected, SDF1-α, T22 and AMD 3100.

- SDF1-α (Stromal cell-derived factor) (Sigma) is a natural ligand of CxCR4. The molecule is composed of 17 amino-acids and binds CxCR4 on the N terminal domain. The interaction SDF1-α / CxCR4 regulates cell migration, proliferation, survival and cancer cell metastasis.

- T22 ([Tyr5,12, Lys7]-polyphemusin II) (Smartox Biotechnoly) is a cationic peptide and an engineered segment derivative of polyphemusin II. T22 binds CxCR4 at Nter and loop extracellular (loop 1 and 2). This peptide inhibits specifically HIV-1 infection mediated by CxCR4.

- AMD3100 a synthetic bis-macrocycle (1,1′-[1,4-Phenylenebis-(methylene)]bis [1,4,8,11-tetraazacyclotetradecane]) (Tocris), is a specific antagonist of CxCR4. This molecule binds CxCR4 on Aspartate Amino Acids #171 and #262 (TM domain). AMD3100 is a “fusion inhibitor of HIV and inhibits tumour growth in cancers.

The solution of SDF1-α was injected at 2 concentrations (10 nM and 20 nM).
The solution of T22 was injected at 3 concentrations (0.8 µM, 1.6 µM and 3.2 µM).
The solution of AMD3100 was injected at 3 concentrations (0.06 µM, 0.125 µM and 0.25 µM).

### Experimental conditions

The interactions between CxCR4 and the ligands (SDF1-α, T22 and AMD3100) were monitored in real time by SPR imaging using the SPRi-Plex and for each injected concentration, the variations of reflectivity representing the quantity of analyte interacting with CxCR4 were determined.
The used running buffer was 50 mM HEPES pH 7.5, 0.05 % BSA.
The flow rate was set to 25 µL/min and the experiment was carried out at 25° C.

Prior to following the interactions, the biochip surface was blocked with 1 % BSA.

## Results and Discussion

### 1. Interaction between CxCR4 and SDF1-α

Figure 4 shows the variation of reflectivity (%) versus time after injection of SDF1-α at 10 nM. The kinetic curve corresponds to an average on the 3 CxCR4 spots, and after subtraction of the signal obtained on the negative control spots. On the different images we can observe that CxCR4 spots are white, whereas the negative control spots remain almost black, which means that there is a specific interaction between CxCR4 and SDF1-α.

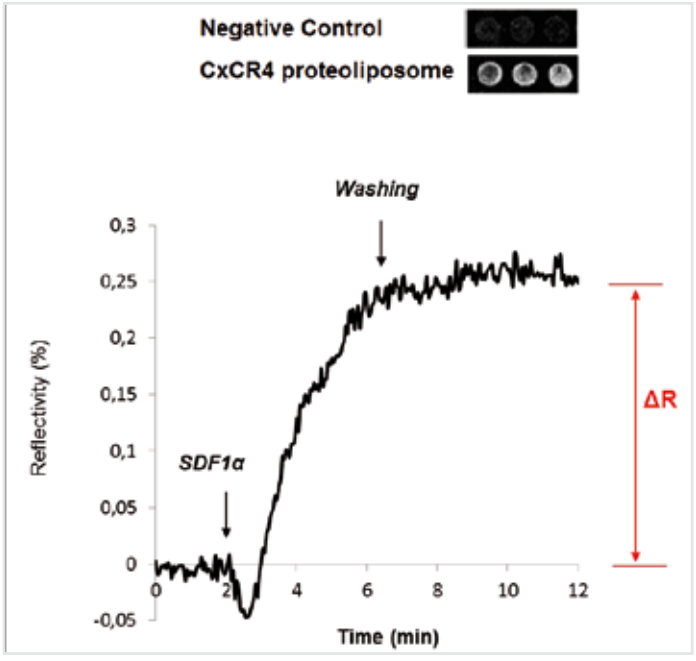


*Figure 4: Kinetic curves obtained after the injection of SDF1-α at 10nM on the CxCR4 spots and difference images on the negative control spots and on the CxCR4 spots.*

Figure 5 indicates the variation of reflectivity after the injection of the SDF1-α solution at 10 nM and 20 nM on the CxCR4 spots and negative control spots. The variations of reflectivity correspond to an average on three spots.

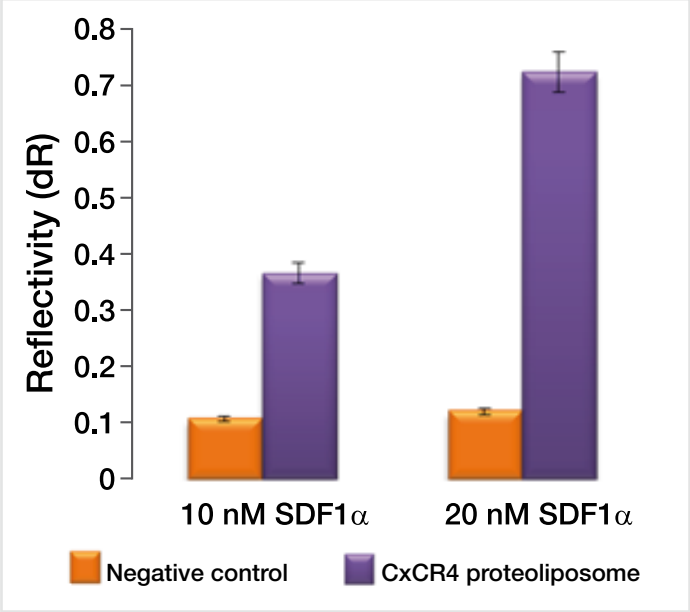


*Figure 5: Variations of reflectivity after injection of SDF1-α at 10 and 20 nM on the negative control spots (red) and on CxCR4 spots (blue).*

These results confirm that the interaction between CxCR4 and SDF1-α is specific.

### 2. Interaction between CxCR4 and T22

Figure 6 represents the variation of reflectivity (%) versus time after injection of T22 at 3 different concentrations, 0.8 µM, 1.6 µM and 3.2 µM on the CxCR4 spots, and on the negtive control spots. The kinetic curve corresponds to an average of 5 spots. On the kinetic curves corresponding to the negative control spots, we can observe a little bit of non specific binding, but we can assert that the interaction between CxCR4 and T22 is specific.

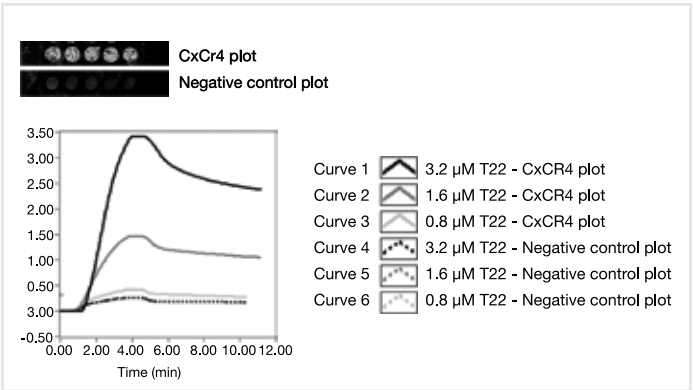


*Figure 6: Kinetic curves after injection of T22 solution at 3 different concentrations (0.8 µM, 1.6 µM and 3.2 µM) on CxCR4 spots and on the negative control spots.*

The graph below (Figure 7) shows the average of the variation of reflectivity on the CxCR4 spots after the three injections of T22, and after subtraction of the signal obtained on the negative control spots.

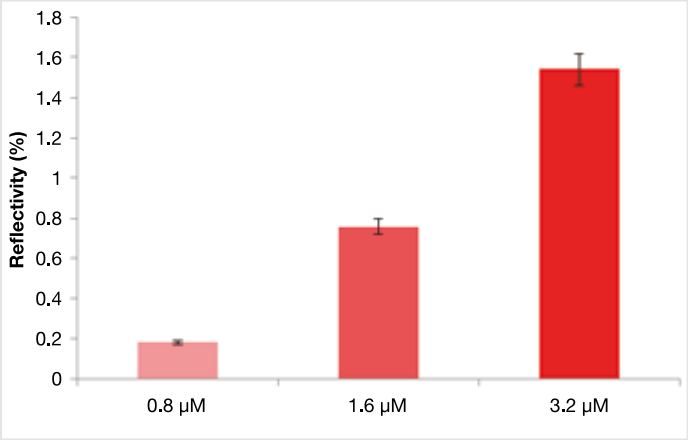


*Figure 7: Variation of reflectivity on CxCR4 spots after injection of T22 at 0.8 µM, 1.6 µM and 3.2 µM, and after subtraction of the SPR signal obtained on the negative control spots.*

On Figure 7 we can observe that the signal is dose-dependent, the variation of reflectivity increases with the concentration of injected T22.

### 3. Interaction between CxCR4 and AMD3100

Figure 8 represents the variation of reflectivity (%) versus time after injection of AMD3100 at 3 different concentrations, 0.06 µM, 0.125 µM and 0.25 µM, on the CxCR4 spots and on the negtive control spots.
The kinetic curve corresponds to an average of 5 spots.

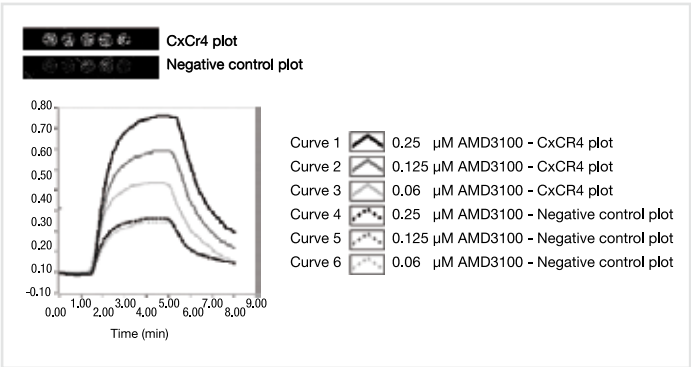


*Figure 8: Kinetic curves after injection of AMD3100 solution at 3 different concentrations (0.06 µM, 0.125 µM and 0.25 µM) on CxCR4 spots and on the negative control spots.*

We observe a weak interaction between AMD3100 and the CxCR4 proteoliposome. The binding of large molecules produces a greater signal while the detection of small molecule ligands as AMD3100 is a challenge with SPR. In order to improve the AMD3100 binding signal we can immobilize a higher protein density on the sensor.

The graph below (Figure 9) shows the average of the variation of reflectivity on the CxCR4 spots after the three injections of AMD3100, and after subtraction of the signal obtained on the negative control spots.

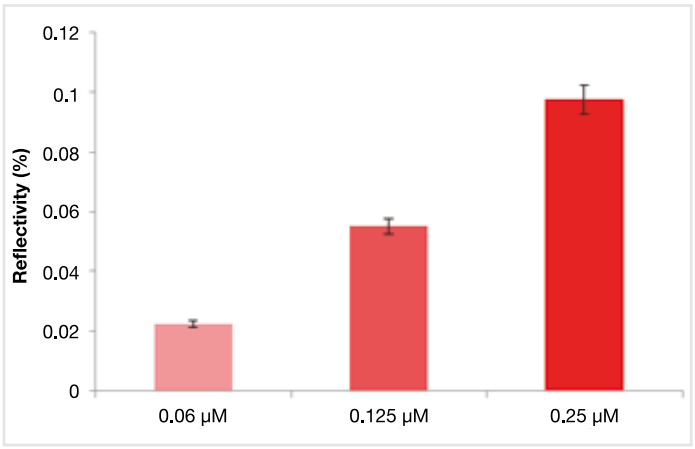


*Figure 9: Variation of reflectivity on CxCR4 spots after injection of AMD3100 at 0.06 µM, 0.125 µM and 0.25 µM, and after subtraction of the SPR signal obtained on the negative control spots.*

On Figure 9 we can observe that the signal is dose-dependent, the variation of reflectivity increases with the concentration of injected AMD3100.

## Conclusion

We demonstrate the interest of SPRi technology for the determination of GPCR-ligand interactions, and independently, of the binding site. These promising results confirm that the SPRi is an useful technique to carry out a primary drug screening and to obtain pharmacokinetic data.



JOBIN YVON Technology

HORIBA Scientific

info.sci@horiba.com www.horiba.com/scientific

**USA:** +1 732 494 8660
**UK:** +44 (0)20 8204 8142
**China:** +86 (0)21 6289 6060
**France:** +33 (0)1 69 74 72 00
**Italy:** +39 2 5760 3050
**Brazil:** +55 (0)11 5545 1500
**Germany:** +49 (0)89 4623 17-0
**Japan:** +81 (0)3 6206 4721
**Other:** +33 (0)1 69 74 72 00